Continuous-Phase Fat Crystals Strongly Influence Water-in-Oil Emulsion Stability

S.M. Hodge and D. Rousseau*

School of Nutrition, Ryerson University, Toronto, Ontario, Canada M5B 2K3

ABSTRACT: To elucidate the role of continuous-phase fat crystals on emulsion destabilization, water-in-canola oil emulsions prepared with 0–2% (w/w) added solid fat (hydrogenated canola stearine or hydrogenated cottonseed stearine) were examined using pulsed NMR droplet-size analysis, sedimentation, and microscopy. Droplet-size analysis showed that addition of either fat prior to emulsification (precrystallized fat) or fat quench-crystallized *in situ* following emulsification (postcrystallized fat) decreased the degree of droplet coalescence, based on volume-weighted (d_{33}) mean droplet diameters, with postcrystallized emulsions being more stable against coalescence. Sedimentation studies corroborated these results, with greatly enhanced stability against sedimentation in postcrystallized emulsions. Precrystallized fat had very little effect on emulsion sedimentation at levels as high as 2% (w/w). Postcrystallized cottonseed stearine produced slightly less resistant emulsions than did canola stearine, even if both were in the β-form. Surface energetics revealed that canola stearine had greater affinity for the oil/water interface and hence a greater displacement energy. The presence of micron-sized (Pickering) crystals located directly at the droplet interface, resulting from *in situ* crystallization or generated by the shearing of precrystallized fats, provided enhanced stability *vis-à-vis* preformed crystals. These stabilized emulsions *via* the formation of crystal networks that partially immobilized droplets.

Paper no. J10898 in *JAOCS 82*, 159–164 (March 2005).

KEY WORDS: Coalescence, fat crystals, interfacial, morphology, polymorphism, water-in-oil emulsion.

The presence of micron-sized fat crystals in oil-continuous systems plays a key role in the kinetic stability of many food systems, namely, tablespreads and numerous confectionary products. In effectively stabilizing the dispersed phase in such mixed systems, fat crystals either entrap dispersed droplets within a network structure or act *via* Pickering stabilization to "encase" droplets in a solid layer (1). This latter phenomenon can be initiated with fat species that either crystallize directly at the droplet interface or diffuse toward the droplet interface as preformed crystals, thereby providing a solid barrier against flocculation, coalescence, and sedimentation (2–4).

In fully elucidating the role that fat crystals play in emulsion stability, it is important to consider the following parameters: their wettability at the oil–water interface (4); the viscoelastic behavior of the interfacial film containing wetted fat crystals (5); and crystal physical properties, including concentration, polymorphism, microstructure, and morphology (6).

The study of colloidal particles as food emulsion-stabilizing agents, and in particular the role of fat crystals, was pioneered in the 1960s by Lucassen-Reynders (1), together with van den Tempel (5). More recently, Johansson, Bergenståhl, and Lundgren (7–11) investigated TG crystals and their effects on emulsion stability. They found that for any given system, there was a destabilizing effect up to a certain critical concentration of crystals, whereas further addition increased stability.

As Pickering species, the role that fat crystals play on emulsion stability strongly depends on how they are wetted by the continuous or dispersed phases (12). During or after emulsification, particles are adsorbed at the interface if it is energetically favorable. Adsorbed particles will be preferentially wetted by either the aqueous or oil phase depending on the composition of the aqueous and oil phases [i.e., the presence and type of emulsifier(s)] as well as the composition and surface properties of the particles. This behavior is described by the contact angle formed at the boundary of the three phases (9), where the contact angle is the angle that the liquid–liquid interface makes to the solid phase as measured through the aqueous phase (Fig. 1). Particles with contact angles smaller than 90° will stabilize oil-in-water (O/W) emulsions. With contact angles greater than 90°, the particles will stabilize water-in-oil (W/O) emulsions (13). If the particles are completely wetted by either the oil or water phase, they become fully dispersed in that phase and will not behave as a Pickering species. The energetics and equilibrium distance associated with the attachment and removal of theoretical spherical particles has been investigated by Levine *et al.* (14) and can provide a means of relating emulsion stability to observed interfacial tensions and contact angle measurements.

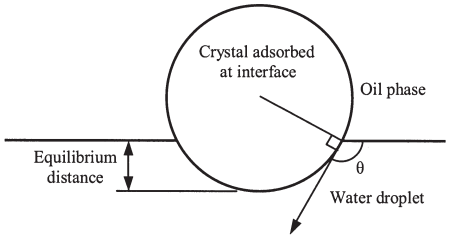

FIG. 1. Schematic representation of a spherical fat crystal adsorbed at the droplet interface in a water-in-oil emulsion.

*To whom correspondence should be addressed at School of Nutrition, Ryerson University, 350 Victoria St., Toronto, ON M5B 2K3, Canada. E-mail: rousseau@ryerson.ca

The aim of this research was to determine the effect of TG fat crystal properties (morphology, polymorphism, and concentration) and interfacial energetics on the stability of a W/O emulsion system using two commonly used fats.

EXPERIMENTAL PROCEDURES

The system studied was a 20% (vol/vol) water-in-canola oil emulsion stabilized with a combination of polyglycerol polyricinoleate (PgPr) emulsifier and various levels of fully hydrogenated canola oil (HCO) or cottonseed oil (HCSO). Distilled water was used, and all other components were of food industry grade; no further purification was performed.

Oil and solid fats. Bleached, deodorized, additive-free canola oil (CO) (Bunge Foods, Toronto, Ontario, Canada) was stored until use under nitrogen at 5°C. The TG composition was determined by GLC (AOCS Method Ce 5-86) (15), with the following modifications: Oven temperature at injection was 70°C followed immediately by ramping to 170°C at 20°C per minute. The ramp rate was then decreased to 15°C per minute and heating continued through to 350°C. The injector temperature was maintained at 5°C above the oven temperature. All species had been eluted by the time 350°C was reached. A 4-m Supelco Petrocol column (0.53 mm i.d.) (Supelco, Oakville, Ontario, Canada) was used with on-column injection in a PerkinElmer AutoSystem XL gas chromatograph (Woodbridge, Ontario, Canada). The most prevalent TG species in canola oil were C_{52} (11.6%), C_{54} (78.5%), and C_{56} (6.2%). The FFA content of the oil, as determined by AOCS Official Method Ca 5a-40 (15), was 0.017%.

The HCO had a capillary melting point of 69.5°C (AOCS Official Method Cc 1-25) (15) and an FFA content of 0.018%. The predominant TG species in HCO were C_{52} (13.3%), C_{54} (73.6%), and C_{56} (5.0%). HCSO had a capillary melting point of 62.5°C and an FFA content of 0.050%. The key TG were C_{50} (16.4%), C_{52} (42.5%), and C_{54} (34.8%).

The solubilities of the solid fats in canola oil were determined by cloud point analysis. This was performed to ascertain the actual level of solid, crystalline fat present in samples prepared using small percentages of solid fat. Both solid fats had solubilities <0.02% (w/w) at 5°C.

X-ray diffraction (XRD). A Rigaku Geigerflex (Danvers, MA) XRD unit (λ = 1.79 Å) was used to determine the powder diffractograms of the solid fats used in the study. Samples were vacuum filtered and analyzed at room temperature (21–24°C). Scans from 1.5 to 35° 2-θ were performed.

Contact angle measurements. Molten HCO and HCSO were crystallized in aluminum weighing boats. The solidified disks of hard fat were then cut into ~1 cm squares and placed in spectrometer cuvettes with the smooth bottom side up. Cuvettes were then filled with either canola oil or canola oil with 0.125% (w/w) PgPr. A small droplet (1 mm o.d.) of water was then injected onto the surface of the solid fat and allowed to age for 24 h. Images of the water droplet were captured with a Teli CCD camera with macro lens assembly and IDS Falcon/Eagle Framegrabber. Image analysis to determine the contact angle of the droplet against the solid surface was performed using SCA 20 version 2.1.5 build 16 (DataPhysics Instrument GmbH, Filderstadt, Germany).

Interfacial tension. The critical micelle concentration of the surfactant in canola oil at room temperature was determined by the break in the interfacial tension vs. log concentration plot. With the PgPr/canola oil/water system, this break occurs at approximately 0.1% as determined by interfacial surface tension measurements against distilled water, using a DuNouy ring tensiometer (Fisher Tensiomat model 21; Fisher Scientific, Nepean, Ontario, Canada). The interfacial tension between water and canola oil at room temperature was 28.8 mN m^{-1}. All emulsions consisted of 0.125% (w/w) surfactant in the continuous oil phase. The interfacial tension between canola oil and water at this concentration of PgPr was 13.4 mN m^{-1} at room temperature. This concentration of emulsifier was expressly chosen because it aided in emulsion formation and imparted an intermediate degree of stability to the emulsion system. Having such a degree of intermediate stability resulted in samples that provided measurable degrees of coarseness through the duration of the experiment. Emulsions that are too fine or that have coalesced too much cannot be characterized as to their droplet size distribution (DSD), thus making comparisons between treatments difficult. Emulsions made without emulsifier were not stable and immediately destabilized.

Microscopy. Polarized light microscopy (PLM) and confocal laser scanning microscopy were used to evaluate the relationship of the water droplets to resolvable fat crystals. A Zeiss Axioplan-2 microscope equipped with a LSM 510 confocal module and the associated software (version 3.2; Zeiss Instruments, Toronto, Ontario, Canada) were used together with a 63× Achroplan water immersion objective. Samples were maintained at 5°C with a TS-60 temperature-controlled stage (Instec Inc., Boulder, CO). Emulsion samples for microscopy purposes were prepared in the usual manner, except that fluorescent dye Rhodamine B (Acros, Ottawa, Ontario, Canada) was added to the water phase at 0.01% (w/w). The dye was excited at 543 nm with the emitted light passing through an LP 560 filter for detection.

Preparation of emulsions. Emulsions were prepared using pre- and postcrystallization regimes, whereby the solid fat was solidified before or after homogenization, with the solid fat representing 0.00, 0.125, 0.25, 0.50, 1.0, and 2.0% (w/w) of the oil phase. Conditions of emulsion preparation were also tailored to produce initial DSD as similar as possible between the two processes.

All emulsions were 20% (vol/vol) water and contained 0.125% (w/w) PgPr in the oil phase. In the precrystallization protocol, solid fat was precrystallized in canola oil (4% w/w) at 25°C under conditions of mild shear for 6 h and subsequently stored at 5°C for 24 h. Appropriate volumes of water, oil, crystal stock solution, and oil with 0.5% (w/w) PgPr were measured and maintained at 5°C during homogenization. The homogenizer (Omni-Mixer Homogenizer; London Scientific, London, Ontario, Canada), which had a micro-attachment containing a blade-type impeller (total cell volume = 5 mL) was operated at

~5000 rpm for 1 min to preblend followed by 2 min at ~27,000 rpm to homogenize.

With the postcrystallized samples, it was essential to homogenize the sample while the high-melting fat was still liquid and, immediately following emulsification, to cool the sample quickly to form the solid fat crystals. The preparation of the postcrystallized samples was performed as follows. A 4% (w/w) solution of the high-melting fat in canola oil was heated to 30°C above the m.p. of the fat used and then maintained at 45°C to prevent recrystallization. Other components used in the preparation of the emulsion were also maintained, combined, and homogenized at this temperature, through the use of a 45°C water bath. After the homogenization regime just described, the homogenization cell was immersed in an ice-water bath and the mixing speed reduced. Mixing was carried out for 6 min, which was determined to reduce the temperature of the contents to 5°C.

Samples were then pipetted into NMR tubes (1 cm o.d.) for NMR droplet size analysis and sedimentation analysis. DSD analyses of the water-in-oil emulsions were carried out using a Bruker Minispec Mq pulsed (pNMR) unit (Bruker Canada, Milton, Ontario, Canada) equipped with a pulsed field gradient unit that allows the characterization of the emulsion DSD in the W/O emulsions. The principle is based on the restricted diffusion of water molecules (16–18). The measurements obtained by the instrument are fit to a unimodal log-normal DSD. DSD samples were analyzed within 15 min of being made. For sedimentation samples, 4 mL was used so as to achieve a sample height of approximately 6 cm. Samples were then capped and placed in a circulating water bath. Samples were prepared in triplicate. A variation to the precrystallization method was also performed, whereby the solid fat was crystallized from the melt in the presence of 0.125% (w/w) PgPr. In this case, the amount of 0.5% (w/w) PgPr canola oil blend used in the preparation of the emulsions was adjusted to maintain a final concentration of 0.125% (w/w) in the final oil phase blend.

RESULTS AND DISCUSSION

Surface phenomena. For particles to stabilize an emulsion droplet effectively, they should ideally be located at the interface, but more so within the continuous phase. Thus, in the case of a W/O emulsion system, the contact angle of the water against the solid body would be greater than 90°. The conditions studied and the observed contact angles are reported in Table 1. Under similar conditions, contact angles with HCO were lower, indicating a slightly greater affinity of the water droplet for canola stearine than for HCSO.

It has been shown that a fat crystal will be wetted by both the water and oil phases if the following condition is true:

$$\gamma_{ow} > \gamma_{os} - \gamma_{sw} \quad [1]$$

where γ_{ow}, γ_{os}, and γ_{sw} are the respective interfacial tensions between the different phases (oil, water, and solid). The resolution of the forces at the junction point is described by Young's equation,

$$\gamma_{ow}\cos\theta = -\gamma_{ow}\cos(180 - \theta) = \gamma_{so} - \gamma_{sw} \quad [2]$$

where θ is the contact angle as measured through the water phase. The interfacial tension between the aqueous and oil phases can be modified through the addition of surfactants and is measured as the force required to deform the interface. However, the solid surface cannot be deformed, so neither γ_{sw} nor γ_{so} can be measured directly. To determine the solid/water or solid/oil interfacial tensions a semi-empirical equation of state (19) may be used:

$$\theta_Y = \frac{(0.015\gamma_{sw} - 2.00)(\gamma_{ow}\gamma_{sw})^{1/2} + \gamma_{ow}}{\gamma_{ow}[0.015(\gamma_{ow}\gamma_{sw})^{1/2} - 1]} \quad [3]$$

where $\cos\theta_Y$ is the Young's angle. Young's angle is the contact angle made by a liquid on a smooth, homogeneous surface of a specified composition and structure. In the current investigation, given the impure nature of the raw materials, it is unlikely that the contact angles observed are in fact Young's. Although the surface is quite smooth, the homogeneity of its structure and composition is unknown. The measured contact angles, Young's equation, and Equation 3 have been used to compile Table 1, which lists the values obtained for the solid/water and solid/oil interfacial tensions.

Given this information, if we consider spherical solid fat particles of radius *r*, the energy associated with this particle when it resides in the continuous oil phase would be

$$4\pi r^2\gamma_{os} \quad [4]$$

As described by Levine *et al.* (14), when this particle is positioned at the interface, the interfacial energy attributed to it will be

$$\pi r^2[2\gamma_{os}(1 - \gamma_{os}\theta) + 2\gamma_{ws}(1 + \cos\theta) - (\gamma_{ow}\sin^2\theta)] \quad [5]$$

TABLE 1
Contact Angles, Calculated Interfacial Tensions, and Displacement Energy for a Spherical Particle of Radius 0.1 μm

Solid phase	Continuous phase	Contact angle	γ_{sw} (mN m^{-1})	γ_{so} (mN m^{-1})	E_{disp}[a] (kT)
Canola stearine	Canola oil	164.9 ± 0.2°	104.3	76.5	262
Canola stearine	Canola oil + 0.125% PgPr[b]	157.1 ± 0.3°	119.2	106.9	636
Cottonseed stearine	Canola oil	172.4 ± 0.8°	104.5	≤75.9	17
Cottonseed stearine	Canola oil + 0.125% PgPr	161.5 ± 0.9°	119.5	106.8	273

[a] $kT = 4.11 \times 10^{-21}$ J.
[b] PgPr, polyglycerol polyricinoleate.

The third term in the brackets represents the area of water/oil interface that is lost owing to the particle's presence at the interface. The difference in the two energies will describe the energy required to displace a particle of a given size from the interface into the continuous phase. By way of example, if we assume spherical particles of radius 0.1 μm with a homogeneous surface, then the energy required to displace them under the conditions mentioned earlier would be as listed in Table 1. A particle of HCO in the presence of emulsifier would require 2.3 times as much energy to displace it from the interface as would a cottonseed stearine particle under the same conditions.

Destabilization of emulsions. Coarsening, or destabilization, of emulsions results mainly from four processes: sedimentation (or creaming), flocculation, coalescence, and Ostwald ripening (20). Of these, the most readily apparent in this study was sedimentation.

Figure 2 shows the visual appearance of post- and precrystallized emulsions after 10 d of storage at 5°C. The white regions of the tubes are composed of the emulsified water droplets and dispersed solid fat crystals whereas the black regions are composed of oil free of either dispersed material. The more stable an emulsion is to sedimentation, the more the sample volume will appear as white. At lower solids levels [i.e., 0.125 and 0.25% (w/w)], postcrystallized samples made with HCO (Fig. 2A) were slightly more resistant to sedimentation than those containing HCSO (Fig. 2B). This coincided with the slightly enhanced resistance of these samples to coalescence, as will be discussed shortly. No samples were completely stable against sedimentation. However, less than 5% supernatant oil was achieved through the addition of a minimum of 0.25% (w/w) HCO or 0.50% (w/w) HCSO. Conversely, with the addition of precrystallized fat, samples sedimented in a very similar fashion, with the exception of cottonseed samples containing 1 and 2% solid fat, which exhibited both sedimentation and a form of creaming, perhaps owing to entrapped air bubbles (Fig. 2D). After 10 d, samples with no solid fat displayed a sediment volume of ~45%. Addition of solid fat up to 2% increased the sediment volume for canola stearine samples to 52% (Fig. 2C), whereas cottonseed stearine resulted in a dispersed phase volume (sedimented and creamed) of 68%.

Evolution of DSD. Regardless of the method of preparation, the initial volume-weighted mean droplet diameter (d_{33}) for all emulsions samples was approximately 4 μm, decreasing slightly with added solids. After 10 d, the d_{33} values increased by varying degrees. Initial d_{00} (geometric mean diameter) values were approximately 4 μm for the precrystallized samples, whereas the initial values for the postcrystallized sample centered at ~2 μm. In both cases, these initial mean diameter values decreased slightly with additional solids. This change in the initial d_{00} values suggests a larger number of small droplets were formed *via* the postcrystallization regime.

Postcrystallization regime. To gauge the degree of coalescence taking place in the samples, a plot was constructed showing the percent change in d_{33} (Fig. 3) from day 0 to day 10 as a function of solid fat addition. An increase in the average droplet size (d_{33}) is evidence of coalescence. Compared with samples containing no added solid fat, a noticeable decrease in the degree of coalescence was observed after a period of 10 d for samples containing either HCO or HCSO. Although coalescence did still occur, the amount observed over 10 d decreased. Stability enhancement was pronounced even at the lowest levels of added solid fat.

Precrystallization regime. Two variations of the precrystallization regime were examined. Both involved crystallizing the solid fat prior to emulsification. One variation involved crystallizing the fat in the presence of PgPr (as would occur with the postcrystallization regime), and the other, crystallizing the fat in pure oil. Little difference was seen between these two treatments. Referring again to the graph of percent change in d_{33} over 10 d, both variations are closely paired for each type of solid fat.

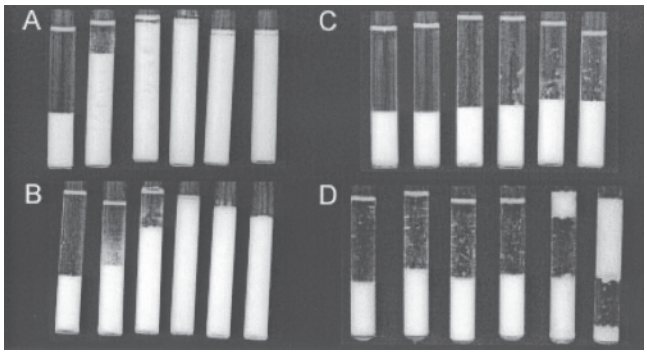

FIG. 2. Emulsions stored for 10 d, containing various levels of (A) postcrystallized canola stearine, (B) postcrystallized cottonseed stearine, (C) precrystallized canola stearine, and (D) precrystallized cottonseed stearine. For each set, the level of solid fat is (left to right): 0, 0.125, 0.25, 0.50, 1.0, and 2.0% (w/w) in the oil phase.

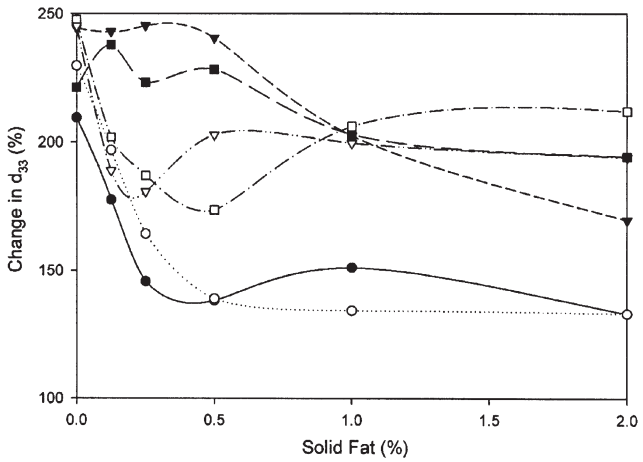

FIG. 3. Percent change in d_{33} from day 0 to day 10. Canola postcrystallized (●), cottonseed postcrystallized (○), canola precrystallized without polyglycerol polyricinoleate (PgPr) (▼), cottonseed precrystallized without PgPr (▽), canola pre-crystallized with PgPr (■), Cottonseed precrystallized with PgPr (□). Error bars omitted for clarity.

At levels of 1 and 2%, both solid fats behaved similarly. At concentrations below 1%, despite some fluctuations in the data trends, overall the HCSO was more effective at decreasing droplet coalescence over a period of 10 d.

Polydispersity. The value sigma (σ) describes the polydispersity of an emulsion's DSD, with larger σ values indicating greater polydispersity. The relationship of σ to the volume-weighted mean (d_{33}) and the number-weighted mean (d_{00}) is expressed as

$$\sigma = \sqrt{\frac{1}{3}\ln\left(\frac{d_{33}}{d_{00}}\right)} \quad [6]$$

Figure 4 shows the evolution in σ for key post- and precrystallized canola and cottonseed samples over time (0, 0.125, and 2% w/w added fat). The precrystallization regime resulted in initial emulsions with narrower size distributions (σ ~ 0.35) than did the postcrystallization regime (σ ~ 0.55). This difference was also observed in samples with no added solid fat, indicating it was not related to any action of solid fat particles, but rather to homogenization conditions. In all cases, σ decreased rapidly over the first 48 h, generally leveling off at longer times. This leveling off was attributed to a narrowing of the DSD, resulting from a large number of very small droplets coalescing during the first day. At all times, values of σ were lower in the precrystallized systems, with the cottonseed system being less polydisperse than the canola, upon addition of 0.125% fat.

Microscopy. Combined brightfield microscopy and PLM were used to understand the role of each of these fats, and the different crystallization regimes, in emulsion stability. For example, Figure 5A shows an emulsion sample, made with 2% postcrystallized cottonseed stearine, aged 10 d. The upper image shows the emulsion droplets and the lower shows the solid fat crystals as resolved by PLM. The droplets are evenly dispersed throughout a fine crystal network. Figure 5B shows an emulsion sample prepared with precrystallized cottonseed stearine. No large spherulites are shown in this field; however, the outline of the droplets is observed in the PLM image as a result of adsorbed crystals.

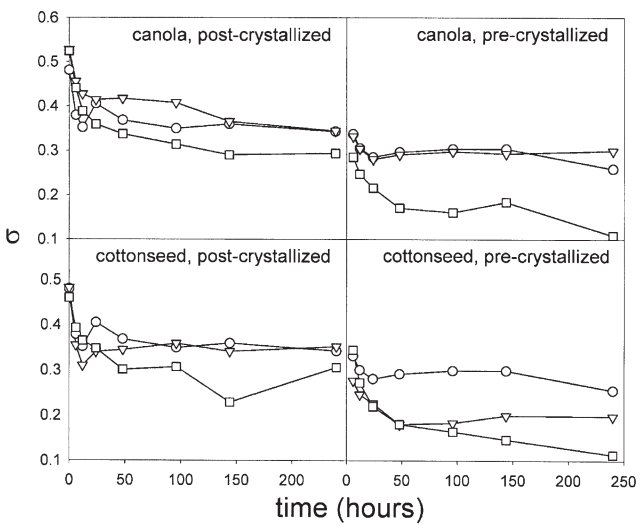

FIG. 4. Evolution of sigma (SD of log normal distribution) for emulsion samples over time. (○) 0, (▽) 0.125, and (□) 2.0% (w/w) solid fat in oil phase. Error bars omitted for clarity.

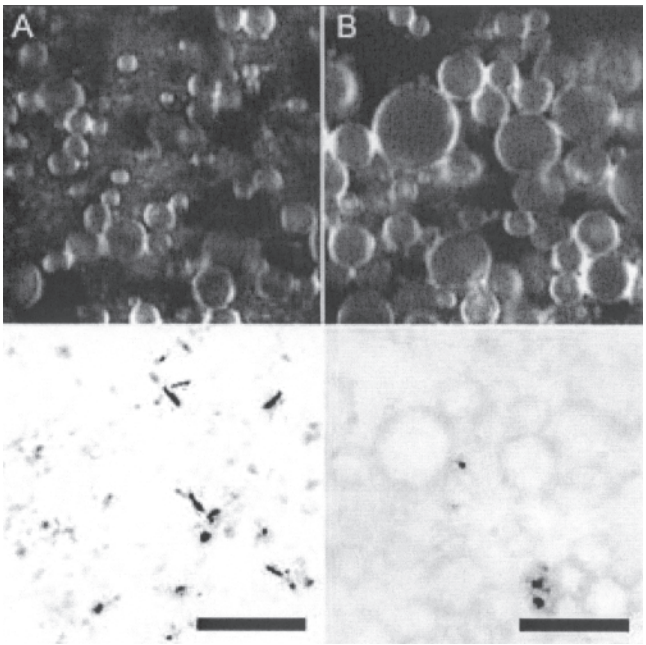

FIG. 5. (Top) Confocal images and (below) corresponding polarized light microscopy images of emulsion samples at 10 d containing 2% (w/w) cottonseed stearine, crystallized (A) after and (B) before emulsification. Scale bar represents 25 μm.

To explain the complicated stabilization of these various emulsions, we must consider the following properties: crystal morphology and size (and associated changes in polymorphism, if any), the affinity of the crystallized fats for the oil/water interface, and their effects on a fat crystal network and Pickering stabilization. To help identify crystal morphology and polymorphism, samples shown in Figure 6 were prepared in an identical fashion to the emulsions with 2% solid fat, but without an aqueous phase. The presence of the aqueous phase in the emulsion would likely influence crystal properties, so the present approach provided us with a simple means to examine crystal properties in detail. Postcrystallized canola and cottonseed stearine (Figs. 6A and 6B, respectively) were similar in appearance. XRD analysis revealed that the cottonseed stearine was in the β polymorph when crystallized in this manner—it is usually a β′-stable fat. Canola crystals were also in the β form, as expected. Despite their near-identical morphology and polymorphism, the canola stearine provided greater stabilization against sedimentation than the cottonseed stearine, as explained earlier. This difference can be attributed to the greater affinity of the canola stearine crystals for the oil–water interface, as previously mentioned.

Figures 6C and 6D show dispersions of precrystallized canola and cottonseed stearine that have been sheared as per the preparation of the emulsions. In this case, the crystals were strikingly different, with the canola fat being present in sharp

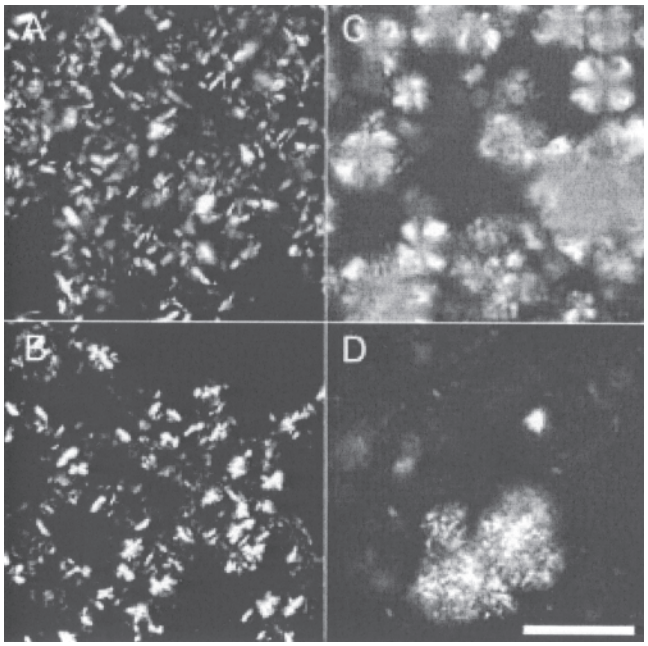

FIG. 6. Dispersions of 2% (w/w) solid fat in canola oil. (A) Postcrystallized canola stearine, (B) postcrystallized cottonseed stearine, (C) precrystallized canola stearine, and (D) precrystallized cottonseed stearine. Scale bar represents 50 μm.

β-tending spherulites and the cottonseed stearine in β′-tending agglomerated platelets, with interspersed small, individual crystal shards. In both fats, crystal agglomerates/spherulites upward of 50 μm in diameter were visible. It is unlikely that these large crystal masses would play any role in Pickering stabilization, given their size relative to the droplets. In all probability, the smaller crystals visible in the cottonseed image were responsible for the enhanced emulsion stability provided to the precrystallized samples at low concentrations (<1% w/w added fat) (Fig. 3), where d_{33} values changed less with the addition of cottonseed than with canola. These smaller crystals would be better suited to provide an adsorbed layer surrounding the droplets. Such adsorbed crystals were not observed in emulsions made with precrystallized HCO. Although stabilization against sedimentation was poor for samples made with either precrystallized fat, the presence of Pickering crystals in HCSO-containing samples enhanced the stability of the emulsions, at least at the microscopic level (change in d_{33}).

In summary, rapid crystallization of the solid fat followed by static storage of the emulsion in the case of the postcrystallized samples favors the formation of a network of fine solid fat crystals, evenly distributed through the continuous phase. Given sufficient interparticle bonds, a fat crystal network can provide a framework or structure to restrict the movement of water droplets, reducing sedimentation, flocculation, and thus coalescence.

On the other hand, emulsions made with precrystallized stearines do not have this refined network structure, as they consist of larger crystals. Owing to the crystallization kinetics, more large crystals and fewer small ones are formed. Consequently, the water droplets and the crystals themselves are freer to migrate, and the result is the compact sediment observed. In all samples, it appears that Pickering stabilization, if observed, is inadequate to visually manifest itself and can only provide stabilization at the microscopic (i.e., changes in d_{33}) level.

REFERENCES

1. Lucassen-Reynders, E.H., Stabilization of Water in Oil Emulsions by Solid Particles, Ph.D. Thesis, Wageningen Agricultural University, Wageningen, The Netherlands, 1962.
2. Hodge, S.M., and D. Rousseau, Flocculation and Coalescence in Water-in-Oil Emulsions Stabilized by Paraffin Wax Crystals, *Food Res. Int. 36*:695–702 (2003).
3. Friberg, S.E., Emulsion Stability, in *Food Emulsions,* 3rd edn., edited by S.E. Friberg and K. Larsson, Marcel Dekker, New York, 1997, pp. 1–56.
4. Pickering, S.U., Emulsions, *J. Chem. Soc. 91*:2001–2021 (1907).
5. Lucassen Reynders, E.H., and M. van den Tempel, Stabilization of Water-in-Oil Emulsions by Solid Particles, *J. Phys. Chem. 67*:731–734 (1963).
6. Ogden L.G., and A.J. Rosenthal, Interactions Between Fat Crystal Networks and Sodium Caseinate at the Sunflower Oil–Water Interface, *J. Am. Oil Chem. Soc. 75*:1841–1847 (1998).
7. Johansson, D., and B. Bergenståhl, Lecithins in Oil-Continuous Emulsions. Fat Crystal Wetting and Interfacial Tension, *Ibid. 72*:205–211 (1995).
8. Johansson, D., and B. Bergenståhl, Wetting of Fat Crystals by Triglyceride Oils and Water. 1. The Effect of Additives, *Ibid. 72*:921–930 (1995).
9. Johansson, D., and B. Bergenståhl, Wetting of Fat Crystals by Triglyceride Oils and Water. 2. Adhesion to the Oil/Water Interface. *Ibid. 72*:933–938 (1995).
10. Johansson, D., B. Bergenståhl, and E. Lundgren, Water-in-Triglyceride Oil Emulsions. Effect of Fat Crystals on Stability, *Ibid. 72*:939–950 (1995).
11. Johansson, D., Weak Gels of Fat Crystals in Oils at Low Temperatures and Their Fractal Nature, *Ibid. 72*:1235–1237 (1995).
12. Darling, D.F., Recent Advances in the Destabilization of Dairy Emulsions, *J. Dairy Res. 49*:695–712 (1982).
13. Schulman, J.H., and J. Leja, Control of Contact Angles at the Oil–Water–Solid Interfaces. Emulsions Stabilized by Solid Particles ($BaSO_4$), *Trans. Faraday Soc. 18*:598–605 (1954).
14. Levine, S., B.D. Bowen, and S.J. Partridge, Stabilization of Emulsions by Fine Particles I. Partitioning of Particles Between Continuous Phase and Oil/Water Interface, *Colloids Surf. 38*:325–343 (1989).
15. *Official Methods and Recommended Practices of the AOCS*, 5th edn., AOCS Press, Champaign, 1997.
16. Tanner, J.E., and E.O. Stejskal, Restricted Self-diffusion of Protons in Colloidal Systems by the Pulsed-Gradient, Spin-Echo Method, *J. Chem. Phys. 49*:1768–1777 (1968).
17. Fourel, I., J.P. Guillement, and D. Le Botlan, Determination of Water Droplet Size Distributions by Low Resolution PFG-NMR: I. "Liquid" Emulsions, *J. Colloid Interface Sci. 164*:48–53 (1994).
18. Fourel, I., J.P. Guillement, and D. Le Botlan, Determination of Water Droplet Size Distributions by Low Resolution PFG-NMR: II. "Solid" Emulsions, *Ibid. 169*:119–125 (1995).
19. Good, R.J., Contact Angles and the Surface Free Energy of Solids, in *Surface and Colloid Science Vol. 2,* edited by R.J. Good and R.R. Stromberg, Plenum Press, New York, 1979, pp. 1–30.
20. Bergenståhl, B., Topics in Food Emulsions, Ph.D. Thesis, Institute for Surface Chemistry, Stockholm, Sweden, and Department of Food Technology, Lund University, Lund, Sweden, 1994.

[Received July 6, 2004; accepted February 8, 2005]